Vol 15 No 7, July 2006
1009-1963/2006/15(07)/1526-06

Chinese Physics

© 2006 Chin. Phys. Soc.
and IOP Publishing Ltd

The viscoelasticity of lipid shell and the hysteresis of subharmonic in liquid containing microbubbles*

Gong Yan-Jun(龚燕君)[a], Zhang Dong(章 东)[a)†], Gong Xiu-Fen(龚秀芬)[a)],
Tan Kai-Bin(谭开彬)[b)], and Liu Zheng(刘 政)[b)]

[a)] *Institute of Acoustics, Nanjing University, Nanjing* 210093, *China*

[b)] *Xinqiao Hospital, Third Military Medical University, Chongqing* 400037, *China*

(Received 17 December 2005; revised manuscript received 2 February 2006)

The viscoelasticity and subharmonic generation of a kind of lipid ultrasound contrast agent are investigated. Based on the measurement of the sound attenuation spectrum, the viscoelasticity of the lipid shell is estimated by use of an optimization method. Shear modulus G_S=10MPa and shear viscosity μ_S=1.49N·S/m^2 are obtained. The nonlinear oscillation of the encapsulated microbubble is studied with Church's model theoretically and experimentally. Especially, the dependence of subharmonic on the incident acoustic pressure is studied. The results reveal that the development of the subharmonic undergoes three stages, i.e. occurrence, growth and saturation, and that hysteresis appears in descending ramp insonation.

Keywords: lipid shell, viscoelasticity, subharmonic, hysteresis
PACC: 4335, 8750C

1. Introduction

Since Gramiak and Shah in 1969 reported the first use of an ultrasound contrast agent (UCA), it has been widely used in the field of medical ultrasound. Microbubbles used as intra-vascular contrast agents can enhance the diagnostic capabilities of ultrasonic imaging, e.g. the detection of flow in small and deep blood vessels, identification of tumours and the imaging of cardiac wall.[1] Additionally, when insonified by an ultrasound at a frequency of f, microbubbles oscillate nonlinearly, and harmonic ($2f$, $3f\ldots$), subharmonic ($f/2$, $f/3\ldots$) as well as ultraharmonic ($3f/2$, $5f/2\ldots$) components are generated, which could be applied for nonlinear harmonic imaging.[2−3] The UCA has extensive therapeutic application beyond diagnosis. The microbubbles in UCA greatly increase the potential for cavitation-related bioeffects, such as cell lysis, thrombolysis, enhancing gene and drug delivery.[4−6]

Usually UCA is a kind of suspension consisting of coated microbubbles with a diameter of less than 10μm, such as Albunex®, Levovist®, Optison®, Definity®, Sonovue®, etc. In order to stabilize the microbubbles to withstand the static pressure and tension effects of the human vasculature, several compounds have been used as microbubble shells or surface-modifying agents, such as acrylates, palmitic acid, phospholipids, albumin and polymers. The viscoelasticity of shell is associated with the microbubble stability, echo emissions, nonlinear oscillations, etc. Consequently, its estimation is essential to the development of UCA. So far, it is difficult to measure directly the viscoelastic parameters by using physical methods. In this work, the estimation of viscoelasticity of the lipid shell is studied for a self-made lipid UCA.[7,8] Based on the measurement of the sound attenuation spectra, the viscoelasticity of the lipid shell is estimated by an optimization method. In addition, ultrasonic subharmonic imaging has recently attracted much attention owing to its ability to provide better CTR (ratio of contrast to tissue) over the fundamental or the second harmonic signals.[3] In order to explore the applications of this lipid UCA in subharmonic imaging, we also investigate the dependence of subharmonic on incident acoustic pressure.

*Project supported by the National Natural Science Foundation of China (Grant Nos 10274032 and 320200265), National Natural Science Foundation of Jiangsu Province, China (Grant No BK2004081).
†E-mail: dzhang@nju.edu.cn

2. Theory and method

2.1. UCA preparation

The preparation of the UCA is performed by lyophilization according to the following steps. (1) Distearoyl phosphatidylcholine (DSPC), dipalmitoylphosphoglycerol (DPPG) and polyethylene Glycol (PEG) are mixed in an appropriate proportion with aqueous solvents. (2) After all the components dissolve, the mixture is poured into 1mL penicillin vials, frozen at –20°C and desiccated at a high pressure. (3) A solvent mixed by hyperosmotic glucose, glycerin and propylene glycol is added into the vials and saturated with C_3F_8 gas. (4) After shaking the vials for 45 seconds, we dilute the solution threefold and pour it into 2mL bottles. (5) After being frozen and lyophilized, a lyophilized powder is obtained for further use. In the experiment, 2mL 0.9% physiological saline is added to the powder in the 2mL bottle, followed by being shaken vigorously to form an emulsion-like solution. Then the solution is diluted to 0.4mg/mL with a concentration of bubbles about 2.0×10^9 microbubbles/mL and the mean radius of the microbubbles being about 1μm.

2.2. Viscoelasticity of lipid shell

Supposing that the interactions of microbubbles can be ignored at low concentrations, the powers absorbed by the UCA specimens is the sum of the power absorbed by the individual bubbles,[9] i.e.

$$\alpha(\omega) = 10\log\int_0^\infty \sigma_{\rm e}(r,\omega)n(r)\mathrm{d}r, \tag{1}$$

where $n(r)$ is the size distribution function of UCA bubbles, $\sigma_{\rm e}(r,\omega)$ is the extinction cross section of a microbubble with a radius r, and given by

$$\sigma_{\rm e}(r,\omega) = 4\pi r^2\frac{c_{\rm L}\delta}{r\omega_0}\frac{\Omega^2}{(1-\Omega^2)^2+\Omega^2\delta^2}, \tag{2}$$

where $c_{\rm L}$ is the sound speed of surrounding liquid, $\omega_0 = \frac{1}{r}\sqrt{\frac{1}{\rho_{\rm L}}\left(3kp_0+12G_{\rm s}\frac{d_{\rm se}}{r}\right)}$ is the resonant angular frequency, p_0 is the atmospheric pressure in the liquid, $\rho_{\rm L}$ is the density of liquid, k is the polytropic exponent of the gas, $d_{\rm se}$ is the thickness of the shell, and $G_{\rm s}$ is the shear modulus. $\Omega = \omega/\omega_0$ is the normalized frequency. The damping constant δ is related to the viscous, thermal and acoustic dampings. As it is mostly dependent on the shell viscosity, we simply set $\delta \approx \delta_{\rm s}$, where $\delta_{\rm s} = 12\mu_{\rm s}d_{\rm se}/(\omega_0\rho_{\rm L}r^3)$, and $\mu_{\rm s}$ is the shear viscosity.

However, it is commonly difficult to directly measure the values of the $G_{\rm s}$ and $\mu_{\rm s}$ by using physical methods. In this work, based on the measurement of acoustic attenuation spectrum, we estimate the viscoelastic shell parameters by using an optimization method. It is assumed that all microbubbles have the same shell parameters $G_{\rm s}$ and $\mu_{\rm s}$. Given initial values of $G_{\rm s}$ and $\mu_{\rm s}$, the sound attenuation spectrum is calculated by Eqs.(1) and (2). The values of $G_{\rm s}$ and $\mu_{\rm s}$ are estimated by adjusting their values to minimize the mean square derivation between the measured and calculated spectra. An ultrasound spectroscopy method[10] is used to measure the acoustic attenuation spectrum. As shown in Fig.1, a broadband acoustic pulse is excited and the signals prior to and during insertion of the specimen are detected and analysed by FFT software. The sound attenuation in specimen can be expressed as

$$\alpha_{\rm s} = \alpha_{\rm w} + \frac{1}{2d}\ln\left(\frac{|P_{\rm w}(\omega)T(\omega)|}{|P_{\rm s}(\omega)|}\right), \tag{3}$$

where $\alpha_{\rm w}$ is the sound attenuation in water; $P_{\rm w}(\omega)$ and $P_{\rm s}(\omega)$ are amplitude spectra before and after the insertion of specimen respectively; $T(\omega)$ is the spectrum of the overall transmission coefficient, with the pulse signal passing through every interface twice taken into consideration; d is the thickness of specimen.

2.3. Nonlinear properties

Insonified by ultrasound, the encapsulated microbubbles in UCA vibrate nonlinearly and its nonlinear oscillation is described by Church's model[9,11]

$$\begin{aligned}&\rho_{\rm L}\left(r''r+\frac{3}{2}(r')^2\right)\\ =&p_0\left(\left(\frac{r_0}{r}\right)^{3\kappa}-1\right)-p_i(t)-4\mu_{\rm L}\frac{r'}{r}\\ &-12\mu_{\rm s}\frac{d_{\rm se}r_0^2}{r^3}\frac{r'}{r}-12G_{\rm s}\frac{d_{\rm se}r_0^2}{r^3}\left(1-\frac{r_0}{r}\right),\end{aligned} \tag{4}$$

where r is the instantaneous radius of the bubble, r', r'' are the first and second time derivatives of the instantaneous radius, r_0 is the equilibrium radius, $d_{\rm se}$ is the shell thickness at rest, $\mu_{\rm L}$ is the shear viscosity in surrounding medium, $p_{\rm i}(t) = p_{\rm A}\cos(\omega t)$ is the time-varying incident acoustic pressure.

A computer program is developed to solve Eq.(1) using a fourth Runge–Kutta algorithm. By use of initial values $r = r_0$ and $r' = 0$ at $t = 0$, the forced oscillation of the microbubble is examined by being excited with a sinusoidal wave. When the incident sound pressure amplitude P_A is not very high, a steady-state solution is obtained. In the present work, we pay attention to the performance of the subharmonic extracted from the spectrum by the FFT software.

3. Results and discussion

3.1. Experimental systems

Figure 1 shows the experimental setup for measuring sound attenuation spectrum. A broadband planar transducer (diameter 15 mm, centre frequency 3 MHz, –6 dB band 1.5 MHz–4.5 MHz, Panametrics, USA) is used as both the transmitter and receiver. An aluminium plate located at a distance of $L = 50$ mm is used to reflect the signal. A sound permeable container with a thickness of $d = 2$ mm is inserted between the transducer and the reflective board, and is about 5 mm close to the latter. A pulser/receiver (Panametrics 5900PR, USA) generates a broadband pulse signal covering frequency range from 1 kHz to 20 MHz. The pulse signal is set to be 1μJ at a pulse repetition frequency of 1 kHz. The received signal is amplified by the pulser/receiver and recorded by a digital oscilloscope (Agilent 54810, USA) with a sampling frequency of 100 MHz/s and a sampling point number of 2048.

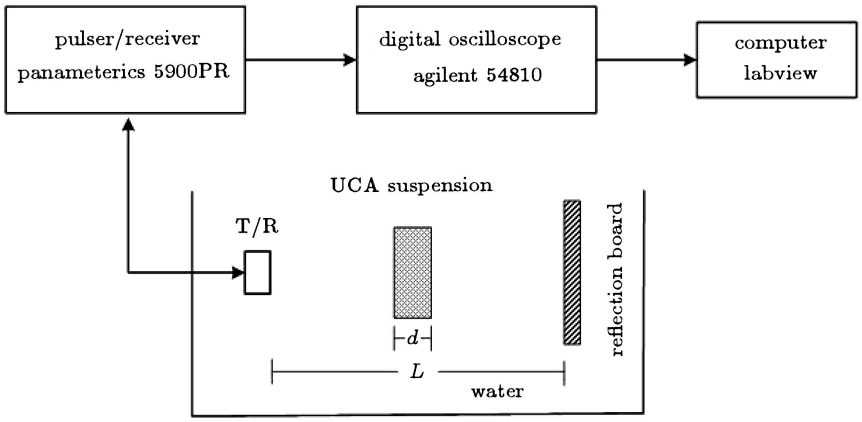


Fig.1. Experimental setup for measuring sound attenuation spectrum.

Figure 2 shows the experimental setup for measuring the subharmonic emissions from UCA. An arbitrary waveform generator (Agilent 33250, USA) is used to generate a 5-MHz burst signal containing 16 cycles at a pulse repetition frequency of 100 Hz. This signal is amplified by an RF power amplifier (ENI 150 A, fixed gain of 55 dB, USA) and then sent to a planar transducer (centre frequency 5 MHz, Panametrics, USA) with a diameter of 15 mm. The response of the bubbles is detected by a needle hydrophone (TNU001A, NTR, USA) located 6 cm from the surface of the transmitter. After passing through a 30-dB preamplifier (NTR, USA), the received signal is recorded by a digital oscilloscope (Agilent 54810, USA) with a sampling frequency of 100 MHz. All measurements are performed at temperature 22°C.

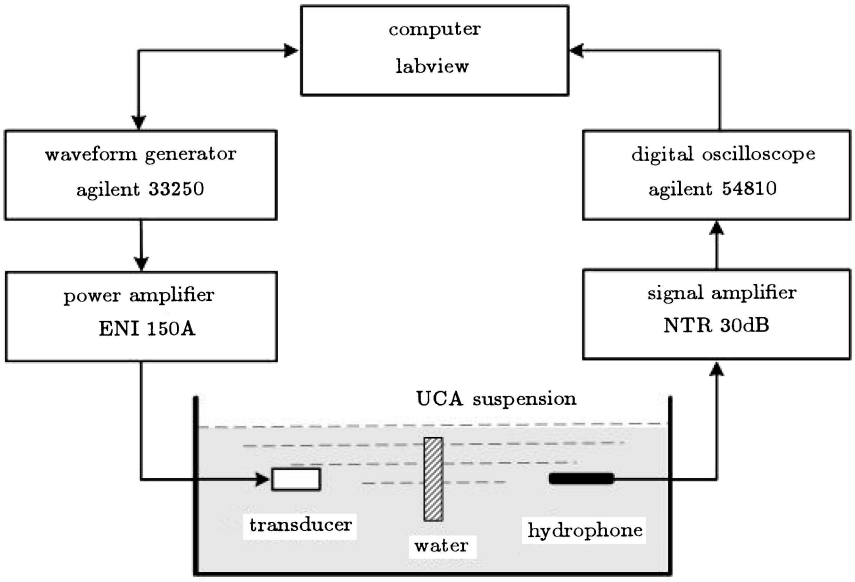


Fig.2. Experimental setup for measuring subharmonic emissions from UCA.

3.2. Results

3.2.1. Viscoelasticity of lipid shell

Figure 3 shows the spectra of the received signals prior to and during the insertion of the UCA specimen. The sound attenuation spectrum is obtained by use of Eq.(3) and plotted in Fig.4 as dots. When the incident frequency is near the resonant frequency of a microbubble, effective absorption of ultrasound energy can be observed. From Fig.4, we estimate that the resonant frequency of the UCA is about 2.3 MHz.

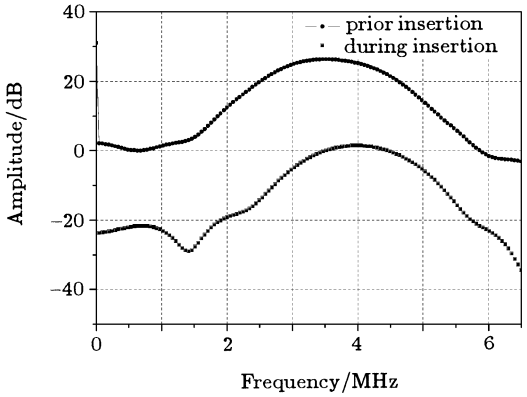


Fig.3. Spectra of receiving signals (a) prior to and (b) during insertion of the UCA specimen.

In order to estimate the values of the viscoelastic shell parameters (G_s and μ_s) from the sound attenuation spectrum, we use an optimization method[12] in which the calculated sound attenuation spectrum is obtained by using Eqs.(1) and (2) with initial values of G_s and μ_s, and compared with the measured one. The values of G_s and μ_s are estimated by adjusting their values to minimize the mean square deviation between the measured and calculated spectra. In our calculation, it is assumed that all microbubbles have the same relative shell thickness d_{se}/r that is about 0.1% of the observed under a microscope. The viscoelasticity of the lipid shell is estimated to be G_s=10 MPa, μ_s=1.49N·S/m^2, and the calculated corresponding sound attenuation spectrum is presented in Fig.4 as solid line in comparison with the measured one.

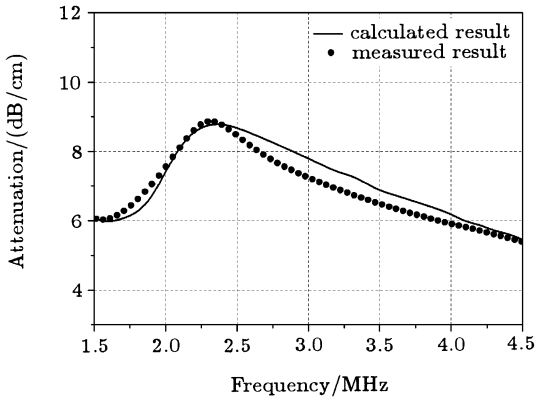


Fig.4. Frequency dependence of attenuation for the UCA specimen.

3.2.2. Subharmonic emissions and hysteresis

By transmitting a 5-MHz tone burst signal, we compare the spectra of the received signals prior to and during insertion of the specimen (normalized to total energy) as shown in Fig.5. It is observed that after insertion of the UCA specimen, the amplitudes

of the high harmonics increase due to nonlinear oscillation of microbubbles, for example, the second harmonic component increases from –43.4 dB to –36.9 dB (by 6.5 dB). Especially, the subharmonic component is observed after insertion of the UCA specimen. It should be noted that two peaks are found near the second harmonic frequency possibly due to the sampling noise.

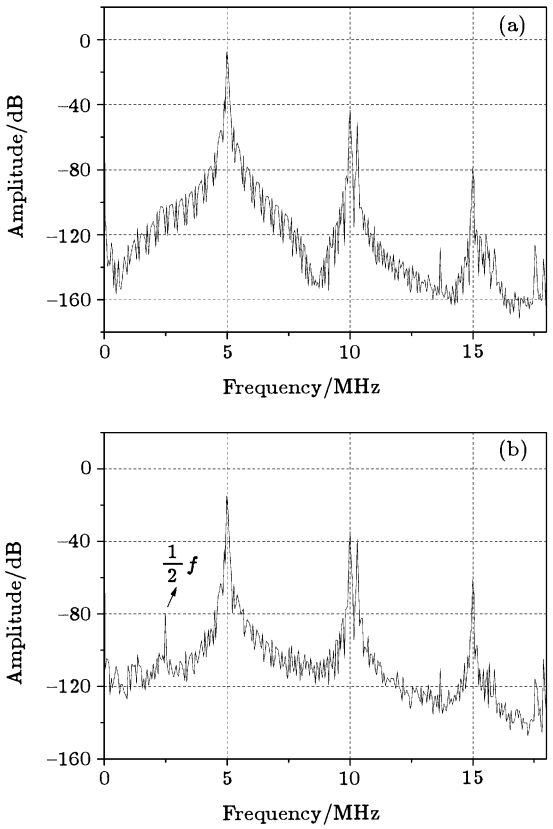


Fig.5. Spectra of the received signals at 0.6-MPa incident pressure (a) prior to and (b) during insertion of the UCA specimen (normalized to total energy).

The dependence of the subharmonic component on the incident sound pressure, predicted by using Eq.(4), is shown in Fig.6. In the numerical calculation, the estimated shell viscoelasticity from the sound attenuation measurement is used and the other parameters are as follows: r_0=1μm, d_{se}/r = 0.1%, p_0=0.101 MPa, κ = 1.09, μ_L=0.001 Pa·S and ρ_L=1kg/m^3. The experimental result of this relationship is also presented in the same figure as dots. The agreement between the measured and calculated results verifies the validity of the estimated shell viscoelasticity. Because the destruction of microbubbles occurs with the increase of the insonating sound pressure, a fresh UCA specimen is used at different sound pressures in order to maintain the number of microbubbles at the same level. It is found that the subharmonic generation could approximately be divided into three stages, i.e. occurrence, growth and saturation, which is in agreement with the results of Sonazoid and Levovist.[13−16] In the occurrence stage (P < 0.4MPa), the subharmonic component is insignificant. In the growth stage (0.4MPa< P <0.8MPa), the subharmonic component grows rapidly. As the sound pressure increases further, the growth of the subharmonic component becomes saturated due to bubble destruction, and the saturation stage (P > 0.8Mp) is reached. The amplitude of the subharmonic component in the saturation stage increases by about 20 dB compared with that in the occurrence stage.

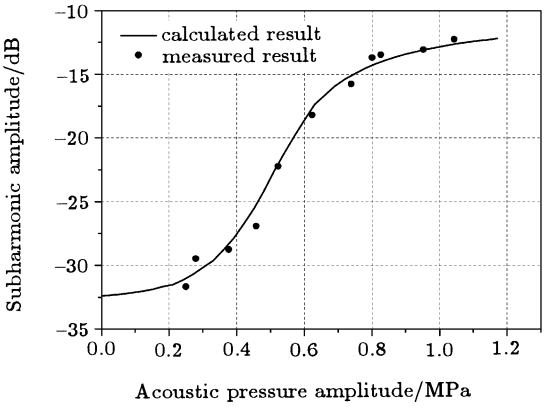


Fig.6. The sound pressure dependence of subharmonic component.

Figure 7 shows the subharmonic component with a rising ramp insonation immediately followed by a reverse of the rising ramp (i.e. descending ramp), where the measured result is given in Fig.7(a) and the predicted one is in Fig.7(b). Here, these two ramps are called mirror ramps. The subharmonic component for the mirror ramps does not overlap and a hysteresis is observed, in which the rising ramp is lower than the descending ramp. This can be explained as follows: (1) More microbubble destruction occurs in the rising ramp over the descending ramp. (2) Enhanced vibration of microbubbles in the rising ramp may result in the leakage of inner gas. A smaller equilibrium radius of microbubble corresponds to a lower threshold of subharmonic component. So the followed descending ramp shifts toward the left. It should be noted that the measured rising ramp in Fig.7 is different from that in Fig.6. In this case only one specimen is used in the whole process and the destruction of microbubbles occurs with the increase of insonating sound pressure. Consequently, the subharmonic component decreases obviously in a high sound pres-

sure range (0.55MPa< P < 0.8MPa) and the saturation stage is reached at P=0.55MPa earlier than at P=0.8MPa in Fig.6.

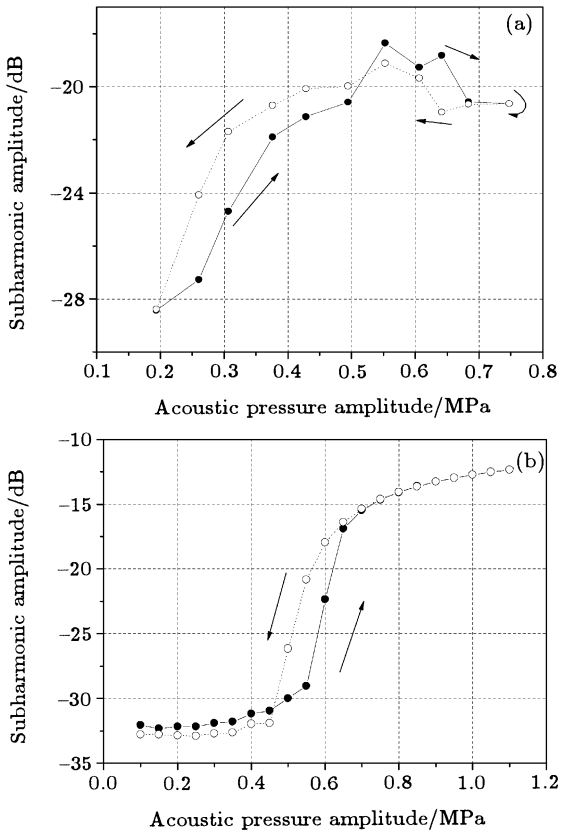


Fig.7. Hysteresis in the curve of sound pressure dependence of subharmonic component. (a) Experimental results; (b) Theoretical results.

The predicted mirror ramps calculated from Eq.(4) are given in Fig.7(b), which coincide qualitatively with the measured ones. Hysteresis is also observed in Fig.7(b), but the subharmonic components in the occurrence stage of the descending ramp are lower than those in the rising ramp, and the subharmonic component in the saturation stage of the rising ramp does not decrease like the behaviour in the measured result. The reason for that is that the theoretical model is based on the single microbubble but not the microbubble clouds.

4. Conclusions

A kind of lipid UCA containing C_3F_8 gas has been studied concerning its viscoelasticity and subharmonic property. The viscoelastic shell parameters (shear modulus and shear viscosity) are estimated from the measurement of acoustic attenuation spectrum. This technique is helpful for the improvement of the performance of UCA. The subharmonic property is studied from the nonlinear oscillation of microbubbles insonified by ultrasound. The results show that the development of subharmonic component is divided into three stages, i.e. occurrence, growth and saturation, and hysteresis appears in the descending ramp insonation owing to the destruction of microbubbles.

References

[1] Goldberg B B, Liu J B and Fersberg F 1994 *Ultrasound in Med. & Biol.* **20** 319
[2] Forsberg F, Goldberg B B, Liu J B, Merton D A and Rawool N M 1996 *J. Ultrasound Med.* **15** 853
[3] Shankar P M, Krishna P D and Newhouse V L 1998 *Ultrasound in Med. & Biol.* **24** 395
[4] Chen W S, Brayman A A, Matula T J and Crum L A 2003 *Ultrasound in Med. & Biol.* **29** 725
[5] Everbach E C and Francis C W 2000 *Ultrasound in Med. & Biol.* **26** 1153
[6] Zderic V, Vaezy S, Martin R W and Clark J I 2002 *Ultrasound in Med. & Biol.* **28** 823
[7] Liu P, Gao Y H, Tan K B, Liu Z and Zou S 2004 *World J. Gastroenterol* **10** 2369
[8] Zhang X, Liu Z, Gao Y H, Zuo S, Tan K B, Bian A N and Zeng G J 2004 *Chin. J. Ultrasound Med.* **20** 247 (in Chinese)
[9] Hoff L, Sontum P C and Hovem J M 2000 *J. Acoust. Soc. Am.* **107** 2272
[10] He P 2000 *J. Acoust. Soc. Am.* **107** 801
[11] Church C C 1995 *J. Acoust. Soc. Am.* **97** 1510
[12] Yu J F, Zhang D, Gong X F, Gong Y J, Zhu Z M and Liu X M 2005 *Chin. Phys. Lett.* **22** 892
[13] Yu J F, Lu R R, Gong X F and Shi W T 2002 *Chin. Phys. Lett.* **19** 1828
[14] Gong Y J, Zhang D and Gong X F 2005 *Chin. Sci. Bull.* **50** 1975
[15] Shi W T, Forsberg F, Raichlen J S, Needleman L and Goldberg B B 1999 *Ultrasound in Med. & Biol.* **25** 275
[16] Lauterborn W 1976 *J. Acoust. Soc. Am.* **59** 283